Pharmacologic inhibition of the CK2-mediated phosphorylation of B23/NPM in cancer cells selectively modulates genes related to protein synthesis, energetic metabolism, and ribosomal biogenesis

Yasser Perera, Seidy Pedroso, Orlando Borras-Hidalgo, Dania M. Vázquez, Jamilet Miranda, et al.

Molecular and Cellular Biochemistry
An International Journal for Chemical Biology in Health and Disease

ISSN 0300-8177

Mol Cell Biochem
DOI 10.1007/s11010-015-2370-x

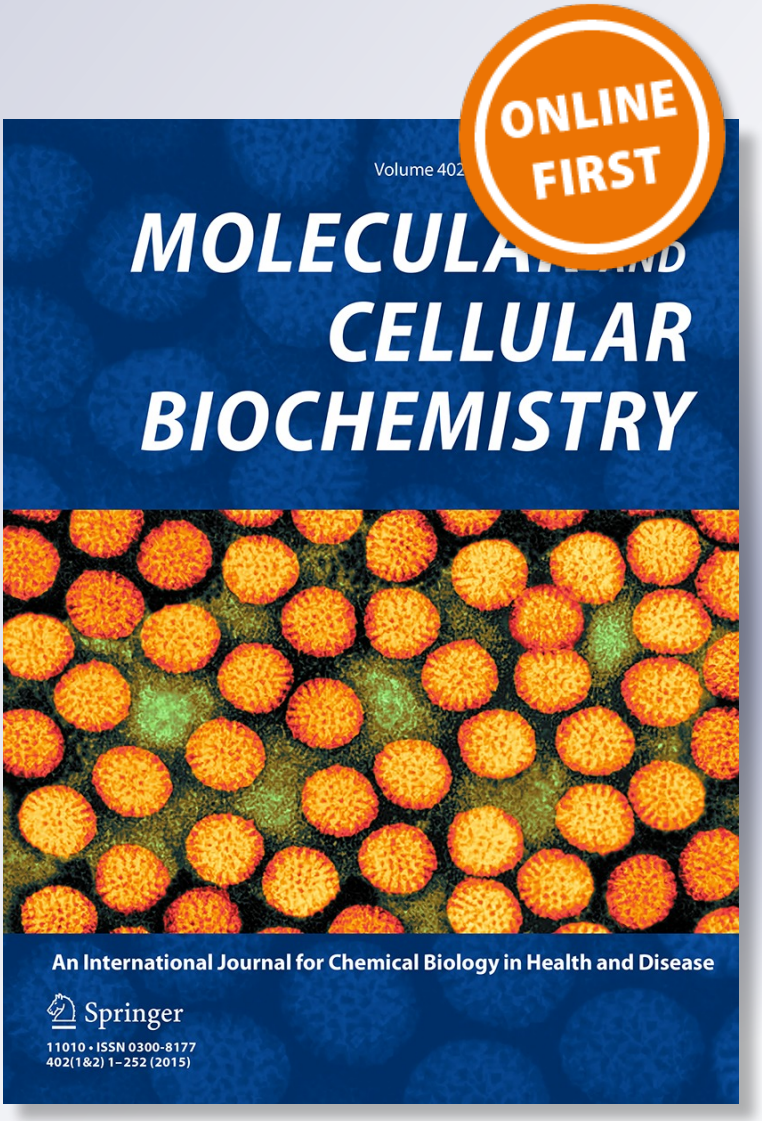

Springer

Mol Cell Biochem
DOI 10.1007/s11010-015-2370-x

Pharmacologic inhibition of the CK2-mediated phosphorylation of B23/NPM in cancer cells selectively modulates genes related to protein synthesis, energetic metabolism, and ribosomal biogenesis

Yasser Perera[1] · Seidy Pedroso[2] · Orlando Borras-Hidalgo[3] · Dania M. Vázquez[2] · Jamilet Miranda[4] · Adelaida Villareal[2] · Viviana Falcón[5] · Luis D. Cruz[6] · Hernán G. Farinas[7] · Silvio E. Perea[1]

Received: 17 November 2014 / Accepted: 23 February 2015

Abstract B23/NPM is a multifunctional nucleolar protein frequently overexpressed, mutated, or rearranged in neoplastic tissues. B23/NPM is involved in diverse biological processes and is mainly regulated by heteroligomer association and posttranslational modification, phosphorylation being a major posttranslational event. While the role of B23/NPM in supporting and/or driving malignant transformation is widely recognized, the particular relevance of its CK2-mediated phosphorylation remains unsolved. Interestingly, the pharmacologic inhibition of such phosphorylation event by CIGB-300, a clinical-grade peptide drug, was previously associated to apoptosis induction in tumor cell lines. In this work, we sought to identify the biological processes modulated by CIGB-300 in a lung cancer cell line using subtractive suppression hybridization and subsequent functional annotation clustering. Our results indicate that CIGB-300 modulates a subset of genes involved in protein synthesis (ES = 8.4, $p < 0.001$), mitochondrial ATP metabolism (ES = 2.5, $p < 0.001$), and ribosomal biogenesis (ES = 1.5, $p < 0.05$). The impairment of these cellular processes by CIGB-300 was corroborated at the molecular and cellular levels by Western blot (P-S6/P-4EBP1, translation), confocal microscopy (JC-1, mitochondrial potential), qPCR (45SrRNA/p21, ribosome biogenesis), and electron microscopy (nucleolar structure, ribosome biogenesis). Altogether, our findings provide new insights on the potential relevance of the CK2-mediated phosphorylation of B23/NPM in cancer cells, revealing at the same time the potentialities of its pharmacological manipulation for cancer therapy. Finally, this work also suggests several candidate gene biomarkers to be evaluated during the clinical development of the anti-CK2 peptide CIGB-300.

Keywords B23/NPM · CK2 inhibitor · CIGB-300 · Nucleophosmin phosphorylation

Introduction

B23/NPM is a multifunctional nucleolar protein frequently overexpressed, mutated, or rearranged in neoplastic tissues [1]. B23/NPM is composed of different functional domains which sustain the ribonuclease and molecular chaperone activities of this protein, as well as its shuttling between the nuclear and cytoplasmic cellular compartments [2–4]. B23/NPM is involved in several cellular processes like ribosome biogenesis, response to stress stimuli, maintenance of

Electronic supplementary material The online version of this article (doi:10.1007/s11010-015-2370-x) contains supplementary material, which is available to authorized users.

✉ Yasser Perera
yasser.perera@cigb.edu.cu

1 Laboratory of Molecular Oncology, Division of Pharmaceuticals, Center for Genetic Engineering and Biotechnology (CIGB), PO BOX 6162, CP10600 Havana, Cuba

2 Department of Genomics, Center for Genetic Engineering and Biotechnology (CIGB), Havana, Cuba

3 Plant Division, Center for Genetic Engineering and Biotechnology (CIGB), Havana, Cuba

4 Bioinformatics Department, Center for Genetic Engineering and Biotechnology (CIGB), Havana, Cuba

5 Chemical-Physical Division, Center for Genetic Engineering and Biotechnology (CIGB), Havana, Cuba

6 Center for Advanced Studies of Cuba (CEAC), Carretera San Antonio, km 1-1/2, Puentes Grandes, Havana, Cuba

7 Laboratory of Molecular Oncology, Quilmes National University, R. Sáenz Peña 352, Bernal B1876BXD, Buenos Aires, Argentina

Published online: 25 March 2015

genomic stability, and regulation of DNA/RNA transcription [5–10]. These diverse roles are mainly regulated by heteroligomer composition and posttranslational modifications, phosphorylation being a major posttranslational event [8, 11–13]. Interestingly, at interphase cells, the major phosphorylatable residue on B23/NPM has been mapped to the casein kinase 2 (CK2)-phosphoaceptor site Ser125 [14, 15]. Such phosphorylation event seems to modulate the dynamic nature of B23/NPM and also contributes to maintain nucleolar integrity in the cell [16, 17].

Unlike most of the CK2 inhibitors which target the catalytic (α or α′) or regulatory subunits (β) of the holoenzyme (αα/ββ), CIGB-300 is a clinical-grade inhibitor that impairs CK2-mediated phosphorylation by targeting the conserved phosphoaceptor domain on CK2 substrates [18, 19]. Interestingly, pulldown experiments in tumor-derived cell lines indicated that B23/NPM is a major target for CIGB-300 in cancer cells [20, 21]. In these experiments, the peptide impaired the CK2-mediated phosphorylation of B23/NPM in a dose-dependent manner, leading to cell death by apoptosis. However, the sequence of events that connect such pharmacological inhibition with the observed cellular demise needs to be clarified.

Using subtractive suppression hybridization (SSH) and subsequent Functional Annotation Clustering of differentially expressed genes [22, 23], we uncover here the biological processes disturbed by pharmacologic inhibition of the CK2-mediated phosphorylation of B23/NPM in cancer cells. Our results indicate that CIGB-300 modulates a subset of genes involved in protein synthesis, mitochondrial metabolism, and ribosomal biogenesis, in agreement with the functional roles ascribed to B23/NPM and with a previous proteomic analysis [24]. Since the enrichment analysis was done at gene level, we further corroborated the impairment of these cellular processes using suitable molecular and cellular markers. Importantly, as CIGB-300 consistently impaired the CK2-mediated phosphorylation of B23/NPM in different tumor cells [21], this peptide becomes a pharmacological tool to assess the potential relevance of such phosphorylation event for cancer cell biology.

Materials and methods

Cell culture and commercial inhibitors

The mycoplasma-free human lung cancer cell line NCI-H125 was originally acquired from the ATCC (Rockville, MD, USA). Cells were routinely cultured in RPMI 1640 (Invitrogen, 11875-119) supplemented with 10 % fetal bovine serum (FBS; PAA, A15-703) and Gentamicin (Sigma, G1264) at 37 °C and 5 % CO_2. In some experiments, the commercial B23 oligomerization inhibitor NSC348884 (Sigma, N3414), the CK2 inhibitor CX-4945 (Selleck Chemicals, S2248), or the mTOR inhibitor RAD001 (Sigma, 07741) were used at selected concentrations.

Sulforhodamine B-based antiproliferative assay

Antiproliferative assays were performed as described previously [25]. Dose–response curves were fitted to the median-effect equation, and the IC_{50} was estimated using the software Calcusyn (Biosoft, Cambridge, UK). Simulated curves were visualized using the software GraphPad Prims v4 (GraphPad Software, San Diego, CA, USA).

Cellular extracts and Western blot experiments

NCI-H125 cells were seeded and cultured as described above. Next day, the cells were incubated with CIGB-300 (100 μM) or vehicle (PBS) during 0.5, 2, or 5 h, or with NSC348884 (5 μM), CX-4945 (5 μM), RAD001 (0.02 μM), and CIGB-300mut (100 μM) during 5 h. The cells were collected by tripsinization, washed with PBS, and lysed in RIPA buffer (#89901) supplemented with protease (#78410) and phosphatase cocktail inhibitors (#78420) from Thermo Scientific (Pierce). The total protein concentration was estimated for each cellular lysate using the Bio-Rad Protein Assay kit (Bio-Rad, 500-0006), and 20 μg/lane of proteins was resolved in conventional SDS-PAGE gels (12.5 %), transferred to nitrocellulose membranes (Amersham Biosciences, RPN203E), and submitted to Western blot experiments using the following antibodies: P-B23/NPM (Ser125) (Abcam, ab109546), B23 (Zymed, 32-5200), S6 (Cell signaling, 2217S), P-S6 (S235/236) (Cell signaling, 4857S), or P-4EBP1 (T37/46) (Cell signaling, 9459). The fluorescent signal was developed using luminol (Sigma, A8511) and registered on X-ray films (Amersham, 28906837). Image analysis from the X-ray films was done with ImageJ 1.37v (NIH, Bethesda, Maryland, USA). Alpha-tubulin protein levels (Cell Signaling, 2144) were used to normalize protein load per lane.

Subtractive suppression hybridization, sequence analysis, and functional annotation clustering

NCI-H125 cancer cells were grown for 20 h and subsequently incubated with 100 μM of CIGB-300 for 30 min. Then, total RNA from CIGB-300-treated or vehicle-treated cells was isolated with Trizol (Invitrogen, 15596-026) and 3 μg was used to synthesize corresponding cDNAs with 200 U of SuperScript II RT (Invitrogen, 18064-014). The dscDNA obtained from CIGB-300-treated (population 1) and PBS-treated (population 2) cells was used as tester and driver, respectively, in a first hybridization (SSH1) and

they were exchanged in a second hybridization (SSH2). This strategy allowed us to obtain CIGB-300's upregulated (SSH1) and downregulated (SSH2) genes in NCI-H125 cells. Both subtractive libraries were constructed using the Clontech PCR-Select cDNA Subtraction kit (Clontech, 637401). The amplified products from both subtraction samples were independently ligated into a pGEMTeasy vector (Promega, A1360) and transformed into *E. coli* strain DH10B. From both libraries, a total of 400 white colonies were randomly selected and inoculated into 96-well plates. The DNA from 378 successfully grown colonies was purified, sequenced, and submitted to Blast analysis using the software Chromas v2.13 (Technelysium Pty Ltd. Australia). Identified genes were submitted to Functional Annotation Clustering using the software DAVID (http://david.abcc.ncifcrf.gov/) [24].

Quantitative real-time PCR

Total RNA was isolated from 3×10^6 CIGB-300-treated or vehicle-treated cells using Tri-reagent (Sigma, T9424). Subsequently, mRNA was obtained and reverse transcribed using the SuperScript III Reverse Transcriptase kit (Invitrogen, 18080-051). Primers to amplify selected genes were designed using Primer3 (http://frodo.wi.mit.edu/primer3/) and preliminarily tested for amplification efficiency and specificity (Online Resource 1) [26]. The absence of genomic DNA contamination in RNA samples was confirmed by qPCR reactions with primers that amplify the *u1a* gene, whereas to verify the absence of qPCR inhibitors, cDNA samples were contaminated with 5×10^3 copies of the pGEMTeasy vector and subsequently amplified with primers (5′-AGCGGATAACAATTTCACACAGGA-3′ y 5′-C GCCAGGGTTTTCCCAGTCACG AC-3′) [27]. All qPCR reactions were performed in triplicate on a Rotor Gene 6000 equipment (Corbett Life Science, UK) using the QuantiTect SYBR Green PCR Kit (Qiagen, 204243) and the following parameters: 95 °C for 15 min, 40 cycles at 95 °C for 15 s, 60 °C for 30 s, and 72 °C for 30 s. The analysis of experimental runs, using Cq and efficiency values, was performed using the Rotor Gene 6000 v1.7 Software (Qiagen, Germany). The putative housekeeping genes (HSKG) *u1a, ywhaz, hmbs,* and *hprt1* were preliminarily assessed to select the best HSKG pair using the Genorm software [28]. Such pair was subsequently used as reference genes for the calculation of relative expression using the REST 2009 v2.0.13 software [29].

Electron microscopy

CIGB-300-treated and vehicle-treated cells were fixed by incubation with a solution containing 4 % formaldehyde (v/v), 0.2 % glutaraldehyde (v/v), 0.1 M phosphate buffer pH 7.3, during 2.5 h at 4 °C. Subsequently, the cells were washed with phosphate buffer, dehydrated by incubation with increasing ethanol concentrations (28–80 % v/v), mixed with Spurr resin, and polymerized during 24 h at 37 °C. Ultrathin sections obtained from each sample were layered onto a cupper grid, stained with a contrast agent, and observed in the transmission electron microscopy MET JEOL JEEM 2000EX. A total of 20 different microphotographs were taken for each experimental variant and subsequently analyzed to evidence nucleolar disassembly.

Mitochondrial membrane potential assay

The JC-1 Mitochondrial Membrane Potential Detection Kit (Cell Technology, JC100) was used to estimate changes in mitochondrial membrane potential by confocal microscopy. JC-1 dual-fluorescence emission was measured after incubating cells with 100 μM of CIGB-300 during 0.5, 1, or 2 h. The experiments were performed using an Olympus FLUOVIEW FV1000 confocal laser scanning microscope (Olympus, Japan) equipped with a LD473 laser source and a BA490-590 detection filter. Images were acquired with an immersion objective UPLSAPO 60xS and subsequently processed using the software Olympus Fluoview v4.0 (Olympus, Japan).

Results

CIGB-300 impairs the CK2-mediated phosphorylation of B23/NPM in lung cancer cells

To identify the genes regulated by CIGB-300 in the lung cancer cell line NCI-H125, first we determined the half maximal inhibitory concentration (IC_{50}) or potency of this peptide using the Sulforhodamine B-based assay (SRB) (Fig. 1a). CIGB-300 exhibited a dose-dependent antiproliferative effect with an estimated IC_{50} of 38.6 μM. Moreover, we also tested the B23/NPM oligomerization inhibitor NSC348884 ($IC_{50} = 1.3$ μM), the CK2 inhibitor CX-4945 ($IC_{50} = 2.9$ μM), the mTOR inhibitor RAD001 ($IC_{50} = 12.4$ μM), and a CIGB-300 mutant peptide which lacks inhibitory activity [21].

Based on these dose–response curves, we selected 100 μM of CIGB-300 to demonstrate by Western blot (WB) that the peptide inhibits the CK2-mediated phosphorylation of B23/NPM using a phosphospecific antibody against the Ser125 residue (Fig. 1b). Additionally, equipotent concentrations of drugs targeting NPM oligomerization, CK2 enzymatic activity, or mTOR activity were also tested in order to assess the specificity of the inhibitory effect. Interestingly, a slight phosphorylation inhibition was observed after 0.5 h of incubation with CIGB-300, whereas a more pronounced

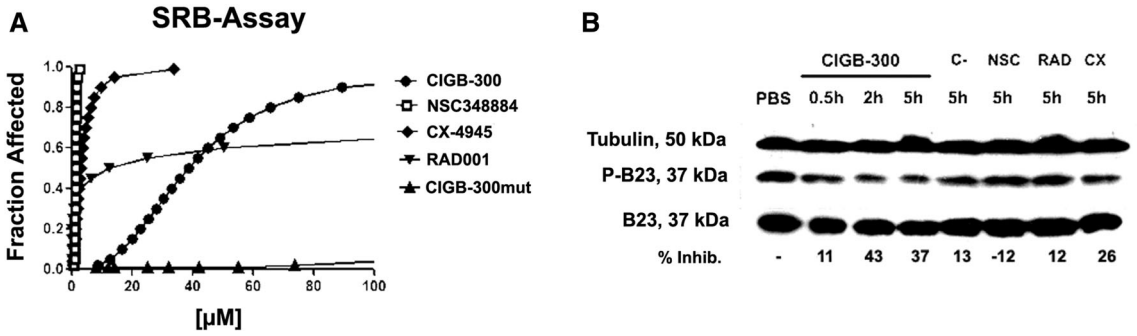

Fig. 1 Inhibitory effects of CIGB-300 peptide and selected small molecule inhibitors over cell proliferation and the CK2-mediated phosphorylation of B23/NPM in NCI-H125 lung cancer cells. **a** CIGB-300, NSC348884, CX-4945, and RAD001 were incubated with NCI-H125 cells during 48 h and their antiproliferative effect determined by the SRB-based assay. Dose–response curves were fitted to the median-effect equation and the potency for each drug (IC_{50}) estimated using the software Calcusyn. **b** Inhibition of B23/NPM's phosphorylation evidenced by Western blot using phosphospecific antibodies against the CK2 phosphoaceptor residue Ser125. The cells were incubated with 100 μM of CIGB-300 during the indicated time intervals. NSC348884, 5 μg/ml; CX-4945, 5 μM; RAD001, 0.02 μM; CIGB-300mut (c−), 100 μM. Alpha-tubulin was used for normalization purposes

effect was registered after 2–5 h of treatment with this peptide (Fig. 1b). On the other hand, only the CK2 inhibitor CX-4945 impaired to some extent the CK2-mediated phosphorylation of B23/NPM after 5 h of treatment, thus confirming the specificity of the observed inhibitory effect.

Identification of CIGB-300 differentially regulated genes in NCI-H125

The subtractive cloning strategy generated 398 clones with cDNA insert sizes ranging from 100 to ~1600 bp (data not shown). The analysis of the corresponding sequences allowed us to identify 48 putative differentially regulated genes in CIGB-300-treated cells (Table 1). The remaining clones comprised sequences without DNA inserts (7 %) or DNA fragments with no significant homology in the database (34 %) (data not shown). Moreover, 19 % of the genes were represented in the library by more than four different clones, whereas six sequences codified for unknown or hypothetical proteins without official gene names assigned (Table 1). Finally, 41 differentially regulated genes were subsequently subjected to functional annotation clustering to identify major biological processes modulated by CIGB-300.

Functional annotation clustering of identified genes

To determine the biological processes more represented or enriched in the SSH library, the obtained gene list was subjected to functional annotation clustering using the DAVID tools. Importantly, 24 of 37 genes with mapped DAVID's ID were clustered to five biological processes: protein synthesis, mitochondrial ATP synthesis, ribosome biogenesis, cell cycle, and regulation of protein metabolism (Fig. 2a; Online Resource 2). Noteworthy, the first three processes included more than 80 % of clustered genes with enrichment scores above the conservative cutoff 1.3 (Fig. 2a).

To verify whether the identified genes were indeed differentially expressed in the presence of CIGB-300, we analyzed the expression levels of a subset of genes by qPCR. A total of 14 genes spanning different annotation clusters and representing roughly 30 % of the SSH library were selected for such expression analysis (Fig. 2b). The results indicated that 11 of the 14 selected genes changed to some extent its expression levels after the incubation of cancer cells with 100 μM of CIGB-300 during 0.5 h. These variations were statistically significant for 4 of the 7 genes included in the top three annotation clusters: protein synthesis (2/4), mitochondrial ATP synthesis (1/1), and ribosome biogenesis (1/2).

Molecular and cellular features of disturbed biological processes

To assess whether CIGB-300 actually impairs the biological processes identified from differentially expressed genes, we evaluated molecular and cellular markers of these processes (Figs. 3, 4). Western blot experiments using phosphospecific antibodies against markers of translational control evidenced that as early as 0.5 h following the addition of CIGB-300, the levels of P-4EBP1 consistently decreased on treated cells, reaching roughly 40 % inhibition after 5 h of incubation (Fig. 3a). Moreover, the levels of P-S6 also decreased under these experimental conditions. However, such inhibition was milder, transient in nature, and well below that observed with CX-4945 and RAD001. As expected, the mTOR inhibitor completely abolished the phosphorylation of S6 and reduced 4EBP1 phosphorylation, which is in line with the localization of both proteins downstream mTORC1 signaling complex (Fig. 3a).

Table 1 CIGB-300's differentially regulated genes identified by SSH in NCI-H125 lung cancer cells after 30 min of treatment with 100 μM of the CIGB-300 peptide

Seq.	Accession[a]	Gene name	Description	Score	*E* value	Recovery frequency[b]
1	gi|86450659|gb|ABC96597.1|	ATP6	ATP synthase F0 subunit 6	153	8.00E−36	24
2	gi|55665435|emb|CAH73371.1|	H3F3A	H3 histone, family 3A	89.4	2.00E−16	17
3	>gi|119380263|gb|ABL73299.1|	COX2	Cytochrome *c* oxidase subunit II	106	1.00E−21	12
4	gi|89243544|gb|AAI14378.1|	–	Unknown (protein for MGC:134704)	140	7.00E−32	12
5	gi|4588085|gb|AAD25980.1|AF095770_1	BBS9	PTH-responsive osteosarcoma D1 protein	52.8	2.00E−05	7
6	gi|119221174|gb|ABL61722.1|	CYTB	Cytochrome *b*	126	2.00E−27	7
7	gi|30585339|gb|AAP36942.1|	ATP5A1	ATP synthase, H+ transporting, mitochondrial F1 complex, alpha sub.	291	3.00E−77	6
8	gi|56181368|gb|AAV83778.1|	NACA	HSD48	212	2.00E−53	5
9	gi|52783077|sp|Q8IVG9|HUNIN_HUMAN	MTRNR2L1	Humanin	50.8	8.00E−05	5
10	gi|62897609|dbj|BAD96744.1|	TUBA1C	Tubulin alpha 6 variant	102	2.00E−20	4
11	>gi|119593494|gb|EAW73088.1|	RPL5	Ribosomal protein L5, isoform CRA_b	183	8.00E−45	2
12	>gi|20381196|gb|AAH27620.1|	RPS6	Ribosomal protein S6	347	4.00E−94	2
13	gi|83282419|ref|XP_729762.1|	–	Senescence-associated protein [Plasmodium yoelii yoelii str.]	89.7	3.00E−19	2
14	gi|12006209|gb|AAG44787.1|AF271776_1	–	DC48	100	6.00E−20	2
15	gi|3123174|sp|Q16465|YZA1_HUMAN	–	Very hypothetical protein	145	2.00E−33	2
16	gi|4506743|ref|NP_001003.1|	RPS8	Ribosomal protein S8	194	6.00E−48	2
17	gi|62897725|dbj|BAD96802.1|	RPL19	Ribosomal protein L19 variant	58.5	4.00E−07	1
18	gi|113201653|gb|ABI33033.1|	ND1	NADH dehydrogenase subunit 1	60.1	1.00E−07	1
19	gi|41471962|gb|AAS07418.1|	DBF4	Unknown	93.6	1.00E−17	1
20	gi|30410790|ref|NP_839952.1|	TUSC3	Tumor suppressor candidate 3 isoform b	149	1.00E−34	1
21	gi|62089150|dbj|BAD93019.1|	UBC	Ubiquitin C variant	179	2.00E−43	1
22	gi|34531284|dbj|BAC86100.1|	FUT1	Unnamed protein product	137	6.00E−31	1
23	gi|33987931|gb|AAH07327.1|	HSP90AB1	HSP90AB1 protein	139	2.00E−31	1
24	gi|5138926|gb|AAD40380.1|	SPCS1	HSPC033	140	1.00E−31	1
25	gi|30584593|gb|AAP36549.1|	GAPDH	Glyceraldehyde-3-phosphate dehydrogenase	294	1.00E−84	1
26	gi|38570357|gb|AAR24619.1|	GNB2L1	Proliferation-inducing gene 21	266	1.00E−69	1
27	gi|62897625|dbj|BAD96752.1|	ACTB	Beta actin variant	180	6.00E−44	1
28	gi|18148478|dbj|BAB83275.1|	–	Core protein, Hepatitis C virus	58.9	6.00E−10	1
29	gi|22538467|ref|NP_002787.2|	PSMB4	Proteasome beta 4 subunit	92.4	2.00E−17	1
30	gi|111072199|emb|CAJ97597.1|	COX1	Cytochrome *c* oxidase subunit I	263	8.00E−69	1
31	gi|90819907|gb|ABD98705.1|	ND4	NADH dehydrogenase subunit 4	110	1.00E−22	1
32	gi|34531176|dbj|BAC86070.1|	–	Unnamed protein product	75.1	4.00E−12	1
33	>gi|119628808|gb|EAX08403.1|	GTF3A	General transcription factor IIIA, isoform CRA_a	94	8.00E−18	1
34	>gi|119608470|gb|EAW88064.1|	RPL7A	Ribosomal protein L7a, isoform CRA_d	305	2.00E−81	1
35	gi|3088339|dbj|BAA25818.1|	RPS11	Ribosomal protein S11	100	9.00E−20	1
36	gi|60299991|gb|AAX18645.1|	ST13	Aging-associated protein 14b	103	1.00E−20	1
37	gi|119621461|gb|EAX01056.1|	RPS7	Ribosomal protein S7, isoform CRA_a	148	2.00E−34	1
38	gi|66911843|gb|AAH96826.1|	DDX24	DDX24 protein	281	2.00E−74	1
39	gi|106322|pir||B34087	–	hypothetical protein (L1H 3′ region)	102	2.00E−20	1
40	>gi|119591124|gb|EAW70718.1|	TUBA4A	Tubulin, alpha 1 (testis specific), isoform CRA_a	54.3	7.00E−06	1
41	gi|2981233|gb|AAC06259.1|	BUB1	Mitotic checkpoint kinase Bub1	90.1	1.00E−16	1
42	gi|119594429|gb|EAW74023.1|	EEF1G	Eukaryotic translation elongation factor 1 gamma, isoform CRA_a	191	3.00E−47	1

Table 1 continued

Seq.	Accession[a]	Gene name	Description	Score	*E* value	Recovery frequency[b]
43	gi|56078799|gb|AAH53371.1|	RPS27	Ribosomal protein S27a	83.6	1.00E−14	1
44	gi|67508866|emb|AJ973596.1|	PQBP1	mRNA for polyglutamine binding protein variant 4	829	0.00E+00	1
45	gi|129395718|gb|EF362804.1|	EEF1A1	EF1a mRNA, complete cds	859	0.00E+00	1
46	gi|5714635|gb|AF159295.1|AF159295	MARK3	Serine/threonine protein kinase Kp78 splice variant CTAK75a mRNA	724	0.00E+00	1
47	gi|206725537|ref|NR_024163.1|	CKS1B	CDC28 protein kinase regulatory subunit 1B (CKS1B), transcript variant 2	919	0.00E+00	1
48	gi|225637497|ref|NR_003286.2|	RN18S1	18S ribosomal RNA (LOC100008588), non-coding RNA	724	0.00E+00	1

[a] BLASTN nr (GenBank + EMBL + DDBJ + PDB sequences)

[b] Number of times each clone was identified in the library

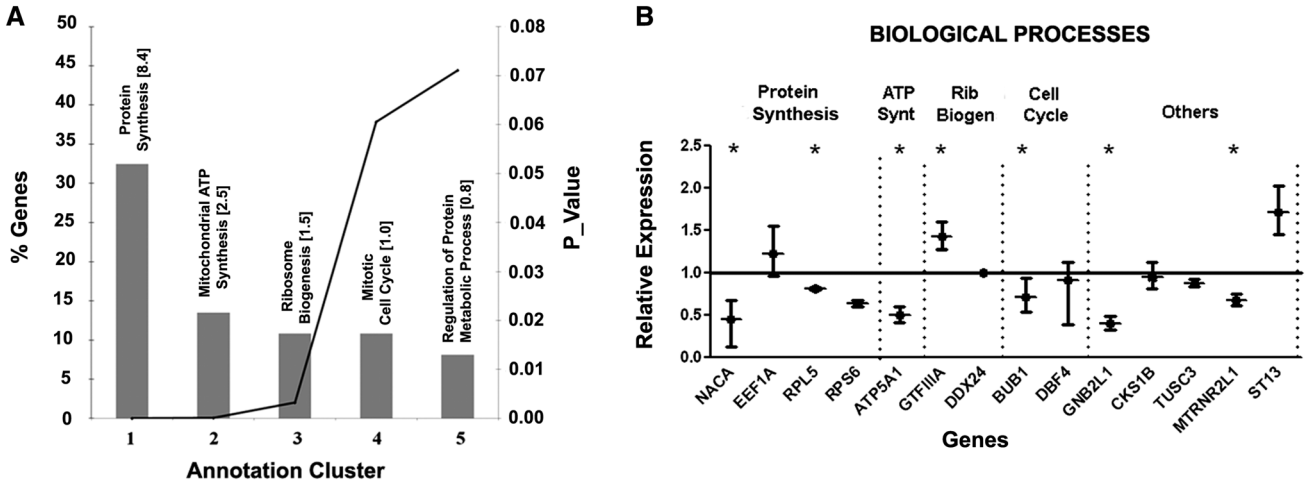

Fig. 2 Biological processes modulated by CIGB-300 and expression analysis of select genes in the NCI-H125 cell line. **a** After sequencing the clones from the SSH library, the final cured identified gene list was submitted to enrichment analysis using the functional annotation clustering tool from DAVID software. The *black solid line* indicates the probability assigned to each annotation cluster, $p < 0.05$ denotes a significant clustering. Values in *brackets* indicate the enrichment scores for each cluster; ES > 1.3 denotes a significant enrichment in genes which participates in the annotated processes. **b** Expression analysis by qPCR of selected genes included in annotation clusters 1–4 ($n = 9$) or connected to other biological processes ($n = 5$) according to **a**. The graph shows changes in relative levels of mRNA for each gene using PBS-treated cells as reference and the HSKG u1a and ywhaz for normalization (mean ± EE). Relative mRNA levels and statistical analysis were performed using the REST software. *Asterisk* significant changes in relative mRNA levels ($p < 0.05$). In all the experiments, the cells were incubated during 0.5 h with 100 μM of CIGB-300. The results shown correspond to one representative of three independent experiments. *EE* standard error

On the other hand, to evidence that CIGB-300 impairs the ribosomal biogenesis, we measured the levels of the ribosomal RNA precursor 45SrRNA by qPCR. Our results demonstrated that CIGB-300 significantly decreases the levels of this precursor rRNA in a time-dependent manner ($p < 0.05$) (Fig. 3b). Moreover, the analysis of the nucleolar structure of CIGB-300-treated cells by electron microscopy also evidenced the impairment of ribosomal biogenesis (Fig. 3c). In such cells, the nucleolar morphology was severely changed from a typical compact structure to fragmented foci.

Taking into account that p53 has been recently involved in a ribosomal biogenesis checkpoint, the levels of p21 and bax mRNA were also measured. After 4 h of incubation with CIGB-300, the levels of the proapototic gene bax decreased ($p < 0.05$), while p21 mRNA levels seemed to increase ($p > 0.05$). Interestingly, the peptide also increased the transcript levels of its own molecular target (B23/NPM), a finding that has been reported for other molecular target therapies [30]. The expression of above-mentioned genes in cells incubated with CIGB-300mut was unaltered, indicating that such changes were not stochastic (Fig. 3b).

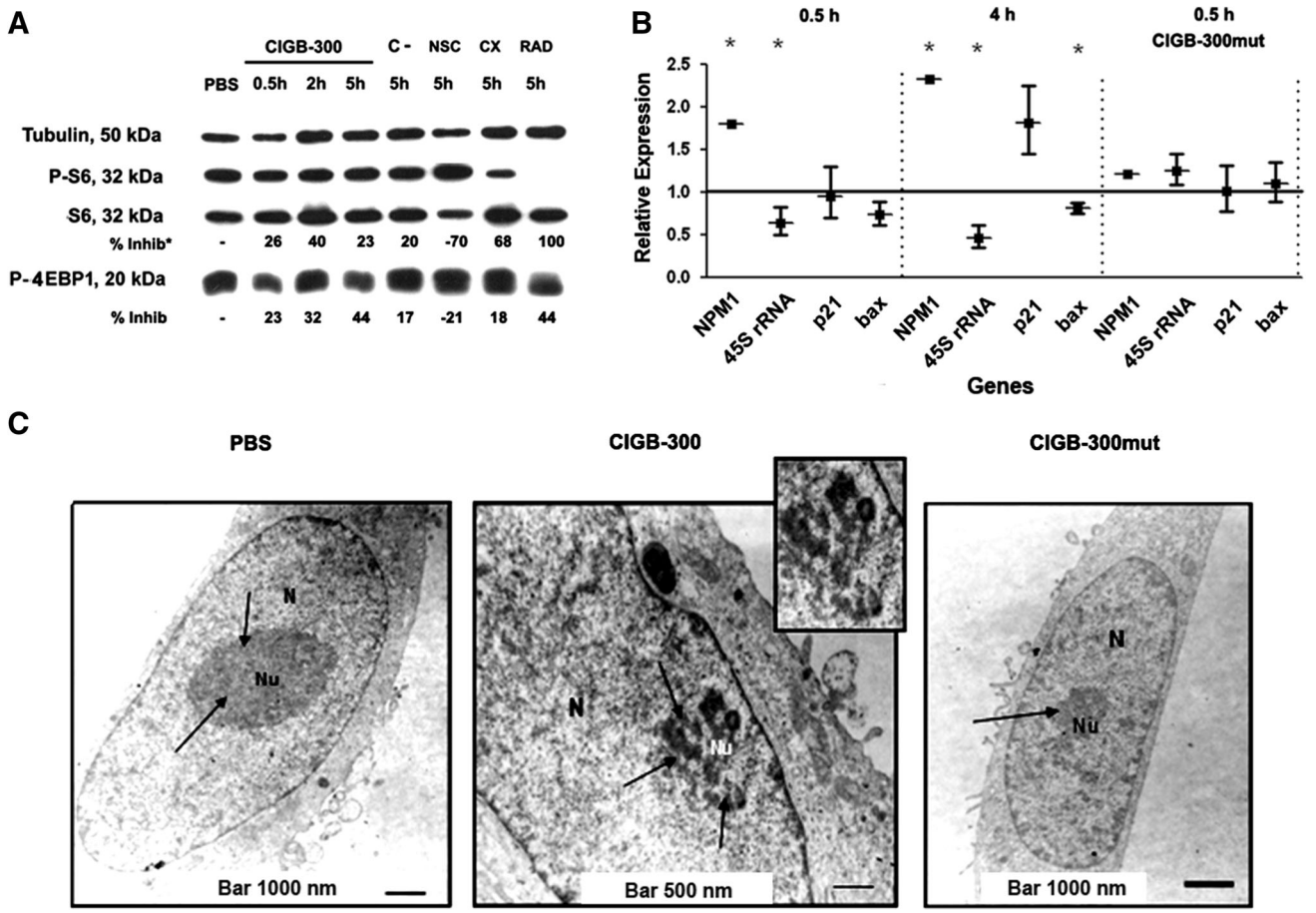

Fig. 3 Detection of molecular and cellular features of disturbed biological processes in NCI-H125 lung cancer cells treated with 100 μM of CIGB-300 during indicated time intervals. **a** Western blot analysis of phosphorylation events connected with translational control downstream of mTORC1 signaling complex. The rest of compounds were used as in (Fig. 1). **b** Changes in the expression levels of genes related to rRNA synthesis, p53- response, and the CIGB-300's target B23/NPM measured by qPCR. Relative mRNA levels and statistical analysis were done as described above. **c** Changes in the nucleolar structure of CIGB-300-treated cells revealed by transmission electron microscopy. The pictures are representative of 20 microphotographs for each sample

Finally, concerning the mitochondrial ATP synthesis, the shifting of the JC-1 red fluorescence toward green fluorescence in CIGB-300-treated cells revealed that this peptide inhibitor disturbed the mitochondrial membrane potential. In these experiments, the cells incubated with CIGB-300 showed a diminished cytoplasmic red fluorescence and a consistent increase in the green signal in the same cellular compartment, when compared to the negative control peptide CIGB-300mut (Fig. 4).

Discussion

While the role of B23/NPM in supporting and/or driving malignant transformation is currently recognized, as far as we know the particular relevance of the CK2-mediated phosphorylation of B23/NPM in this cellular context remains unsolved [1, 31, 32]. Pioneering in vitro experiments conducted by Szebeni et al. demonstrated that B23/NPM displays molecular chaperone activities which depend on CK2 phosphorylation [33]. Subsequent genetic experiments comprising the substitution of the CK2 phosphorylatable residue on B23/NPM evidenced that such phosphorylation modifies the nuclear protein dynamics and the nucleolar structure of the cell [16, 17].

Altogether, these findings pointed out to a role for the CK2-mediated phosphorylation of B23/NPM in ribosomal biogenesis, probably by modulating its molecular chaperone activity at the different stages where it seems to be involved [5, 34, 35]. However, as B23/NPM is a multifunctional protein which is involved in several cellular functions, we aimed to identify the full array of biological processes modulated by the pharmacologic inhibition of this major posttranslational event [11]. At the same time, we expected to gather new molecular and cellular clues

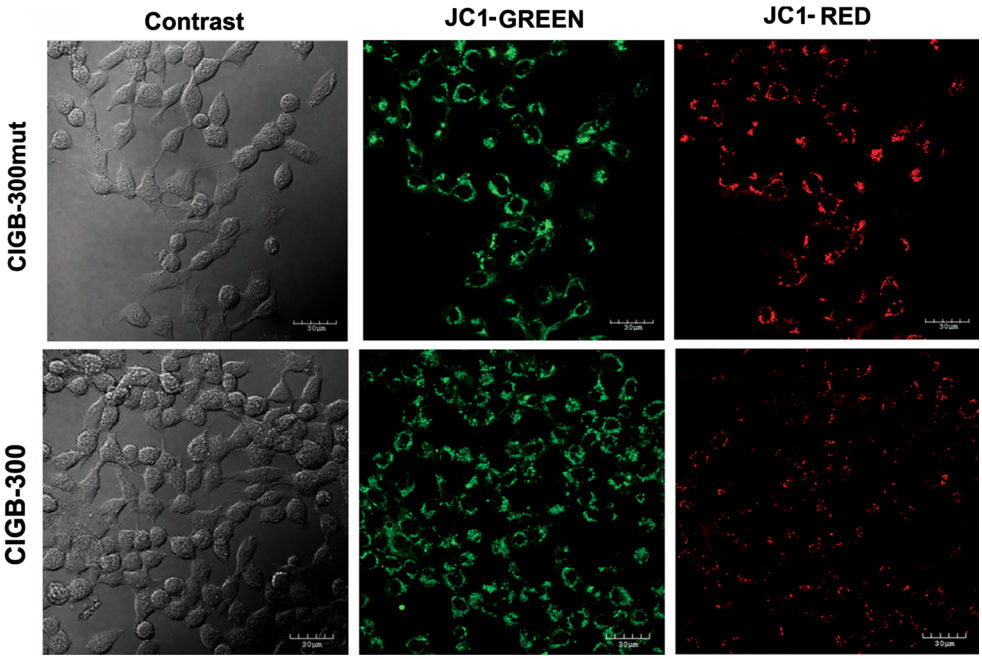

Fig. 4 Mitochondrial impairment in NCI-H125 lung cancer cells after short-term treatment with CIGB-300. JC-1 fluorescence emission in the *Red* and *Green* channel was registered by confocal microscopy after 1 h of incubation with 100 μM of CIGB-300 or the control peptide CIGB-300mut. *Inserted bar* 30 μm. (Color figure online)

that help explain the cellular demise that follows CIGB-300 incubation with tumor cells [19–21].

Firstly, we demonstrated that CIGB-300 but not the B23 oligomerization inhibitor NSC348884, the mTORC1 inhibitor RAD001 or the control peptide CIGB-300mut, significantly impairs the CK2-mediated phosphorylation of B23/NPM. Otherwise, the inhibitory effect of the CK2 inhibitor CX-4945 over the phosphorylation of this particular substrate was mild, which is in line with a previous report [36]. Having demonstrated that CIGB-300 inhibited the CK2-mediated phosphorylation of B23/NPM, we generated the SSH library to identify differentially regulated genes in CIGB-300-treated lung cancer cells.

Functional annotation clustering analysis indicated that CIGB-300 impairs protein synthesis. Roughly 30 % of the identified genes clustered to such biological processes with enrichment scores (ES) above the recommended value (ES $>$ 1.3) [24]. Therefore, to corroborate at the molecular level the disturbance of protein synthesis, we used two established markers, the downstream mTOR signaling proteins 4EBP1 and S6 [37, 38]. In agreement with the identification of protein synthesis as a cellular process modulated by CIGB-300, we observed a partial inhibition of the phosphorylated 4EBP1. As hypophosphorylated 4E-BP1 strongly interacts with eIF4E thus preventing protein translation, such finding corroborates the disturbance of this cellular process by CIGB-300. Interestingly, under the same experimental conditions P-S6 protein levels only marginally/transiently decreased. Considering that S6 phosphorylation by S6K correlates with 5′TOP mRNAs translation, which includes components of the translational machinery and the B23/NPM target itself [39], a compensatory feedback loop might explain this particular finding. Overall, our results suggest that CIGB-300 and the related inhibitors NSC348884 and CX-4945 could affect protein synthesis at different levels, thus uncovering mechanistic differences between these inhibitors.

CIGB-300 also modulated ribosome biogenesis in NCI-H125 cancer cells. This finding was somehow expected since B23/NPM has been involved in three of the four major steps of such cellular processes. B23/NPM participates in the Pol I-mediated transcription of the precursor 45S-rRNA molecule, its subsequent maturation and ribosome subunit export to the cytoplasm [5, 34, 35]. Of note, we demonstrated by qPCR that CIGB-300 significantly decreased the levels of 45S-rRNA. As the synthesis of such precursor rRNA constitutes the rate-limiting step of ribosomal biogenesis, this finding corroborates that the CIGB-300 peptide is impairing the ribosomal biogenesis [40]. Such notion was further reinforced by the loss of the nucleolar structure in CIGB-300-treated cells, an effect already reported for this peptide [20]. Moreover, the observed induction of p21 in these cells may also indicate the activation of a ribosome biogenesis checkpoint which results in p53 protein stabilization following a nucleolar stress [41]. In NCI-H125 cells, such induction was probably mild since this cell line harbors a mutated p53 with residual DNA binding activity [42]. Overall, our results with CIGB-300 parallel to some extent those obtained by Louvet et al. using the phosphomutant construct S125A B23/NPM in HeLa cells [17].

Ribosome biogenesis is a demanding cellular process which consumes 80 % of cellular energy [43]; hence, it is tempting to speculate that the observed regulation of the ATP mitochondrial metabolism may be linked to its impairment. Both, JC-1 and the previously reported prohibitin marker [24], corroborated disturbances at the mitochondrial membrane potential which may explain the identification of the Mitochondrial ATP Synthesis as a biological processes modulated by CIGB-300.

Although gene transcription and proteomic profiles usually display low degree of correlation [44], the functional annotation clustering of SSH-identified genes showed considerable overlap with a previous proteomic study [24]. Remarkably, both at gene and protein levels, protein synthesis and ribosomal biogenesis were identified as biological processes modulated by CIGB-300 in cancer cells. As ribosomal biogenesis builts the translational machinery, which ultimately determines cell growth and proliferation, its pharmacological inhibition could explain the antineoplastic effect of CIGB-300 in tumor cells.

Despite the fact B23/NPM has been proposed as a major target for CIGB-300 in solid tumors, at present we cannot completely rule out this peptide may also blocks the phosphorylation of other CK2 substrates. Particularly, in the cell nucleolus at least other five CK2 substrates with functional roles in ribosomal biogenesis have been reported [45]. This raises the possibility that others, yet unidentified CIGB-300's targets, might also contribute to the observed cellular phenotype.

Finally, our results also provided potential candidate gene biomarkers, which have been mechanistically connected to CIGB-300's antineoplastic effect, could represent suitable pharmacodynamic biomarkers for the clinical development of this anti-CK2 peptide (i.e. NACA, GTFIIIA, 45SrRNA, NPM). Importantly, the suitability of the above-proposed gene biomarkers needs to be explored in further preclinical models and ultimately validated in human clinical trials.

Acknowledgments This work was supported by C.I.G.B. and Biorec: Grant CIGB-300.

Conflict of interest The authors declare no conflict of interests.

References

1. Grisendi S, Mecucci C, Falini B, Pandolfi PP (2006) Nucleophosmin and cancer. Nat Rev Cancer 6:493–505
2. Borer RA, Lehner CF, Eppenberger HM, Nigg EA (1989) Major nucleolar proteins shuttle between nucleus and cytoplasm. Cell 56:379–390
3. Yun JP, Chew EC, Liew CT, Chan JY, Jin ML, Ding MX, Fai YH, Li HK, Liang XM, Wu QL (2003) Nucleophosmin/B23 is a proliferate shuttle protein associated with nuclear matrix. J Cell Biochem 90:1140–1148
4. Hingorani K, Szebeni A, Olson MOJ (2000) Mapping the functional domains of nucleolar protein B23. J Biol Chem 275: 24451–24457
5. Murano TK, Okuwaki M, Hisaoka M, Nagata K (2008) Transcription regulation of the rRNA gene by a multifunctional nucleolar protein, B23/nucleophosmin, through its histone chaperone activity. Mol Cell Biol 28:3114–3126
6. Wu MH, Yung BYM (2002) UV Stimulation of nucleophosmin/B23 expression is an immediate-early gene response induced by damaged DNA. J Biol Chem 277:48234–48240
7. Li J, Zhang X, Sejas DP, Bagby GC, Pang Q (2004) Hypoxia-induced nucleophosmin protects cell death through inhibition of p53. J Biol Chem 279:41275–41279
8. Zhang H, Shi X, Paddon H, Hampong M, Dai W, Pelech S (2004) B23/nucleophosmin serine 4 phosphorylation mediates mitotic functions of polo-like kinase 1. J Biol Chem 279:35726–35734
9. Takemura M, Sato K, Nishio M, Akiyama T, Umekawa H, Yoshida S (1999) Nucleolar protein B23.1 binds to retinoblastoma protein and synergistically stimulates DNA polymerase alpha activity. J Biochem 125:904–909
10. Dhar SK, Lynn BC, Daosukho C, St. Clair DK (2004) Identification of nucleophosmin as an NF-κB co-activator for the induction of the human SOD2 gene. J Biol Chem 279:28209–28219
11. Okuwaki M (2008) The structure and functions of NPM1/nucleophsmin/B23, a multifunctional nucleolar acidic protein. J Biochem 222:1–7
12. Okuda M, Horn HF, Tarapore P, Tokuyama Y, Smulian AG, Chan PK, Knudsen ES, Hofmann IA, Snyder JD, Bove KE, Fukasawa K (2000) Nucleophosmin/B23 is a target of CDK2/cyclin E in centrosome duplication. Cell 103:127–140
13. Okuwaki M, Tsujimoto M, Nagata K (2002) The RNA binding activity of a ribosome biogenesis factor, nucleophosmin/B23, is modulated by phosphorylation with a cell cycle-dependent kinase and by association with its subtype. Mol Biol Cell 13:2016–2030
14. Chan PK, Liu QR, Durban E (1990) The major phosphorylation site of nucleophosmin (B23) is phosphorylated by a nuclear kinase II. Biochem J 270:549–552
15. Jiang PS, Chang JH, Yung YB (2000) Different kinases phosphorylate nucleophosmin/B23 at different sites during G(2) and M phases of the cell cycle. Cancer Lett 153:151–160
16. Negi S, Olson MO (2006) Effects of interphase and mitotic phosphorylation on the mobility and location of nucleolar protein B23. J Cell Sci 401:616–620
17. Louvet E, Junera HR, Berthuy I, Hernandez-Verdun D (2006) Compartmentation of the nucleolar processing proteins in the granular component is a CK2-driven process. Mol Biol Cell 17:2537–2546
18. Cozza G, Pinna LA, Moro S (2013) Kinase CK2 inhibition: an update. Curr Med Chem 20:671–693
19. Perea SE, Reyes O, Puchades Y, Mendoza O, Vispo NS, Torrens I, Santos A, Silva R, Acevedo B, López E, Falcón V, Alonso DF (2004) Antitumor effect of a novel proapoptotic peptide that impairs the fosforilación by the protein kinase 2 (casein kinase 2). Cancer Res 64:7127–7129
20. Perera Y, Farina HG, Gil J, Rodriguez A, Benavent F, Castellanos L, Gómez RE, Acevedo BE, Alonso DF, Perea SE (2009) Anticancer peptide CIGB-300 binds to nucleophosmin/B23, impairs its CK2-mediated phosphorylation, and leads to apoptosis through its nucleolar disassembly activity. Mol Cancer Ther 8:1189–1196
21. Perera Y, Costales HC, Diaz Y, Reyes O, Farina HG, Mendez L, Gómez RE, Acevedo BE, Gomez DE, Alonso DF, Perea SE (2012) Sensitivity of tumor cells towards CIGB-300 anticancer peptide relies on its nucleolar localization. J Pept Sci 18:215–223

22. Diatchenko L, Lau YF, Campbell AP, Chenchik A, Moqadam F, Huang B, Lukyanov S, Lukyanov K, Gurskaya N, Sverdlov ED, Siebert PD (1996) Suppression subtractive hybridization: a method for generating differentially regulated or tissue-specific cDNA probes and libraries. Proc Natl Acad Sci 93:6025–6030
23. Huang DW, Sherman BT, Lempicki RA (2009) Systematic and integrative analysis of large gene lists using DAVID bioinformatics resources. Nat Protoc 4:44–57
24. Rodriguez-Ulloa A, Ramos Y, Gil J, Perera Y, Castellanos-Serra L, Garcia Y, Betancourt L, Besada V, Gonzalez LJ, Fernandez-de-Cossio J, Sanchez A, Serrano JM, Farina HG, Alonso DF, Acevedo BE, Padron G, Musacchio A, Perea SE (2010) Proteomic profile regulated by the anticancer peptide CIGB-300 in non-small cell lung cancer (NSCLC) cells. J Proteome Res 9:5473–5483
25. Boyd MR (1997) The NCI in vitro anticancer drug discovery screen: concept, implementation, and operation, 1985–1995, in anticancer drug development guide: preclinical screening, clinical trials, and approval. Humana Press, Totowa, pp 23–42
26. Rozen S, Skaletsky H (2000) Primer3 on the WWW for general users and for biologist programmers. Methods Mol Biol 132:365–386
27. Nolan T, Hands RE, Bustin SA (2006) Quantification of mRNA using real-time RT-PCR. Nat Protoc 1:1559–1582
28. Vandesompele J, De Preter K, Pattyn F, Poppe B, Van Roy N, De Paepe A, Speleman F (2002) Accurate normalization of real-time quantitative RT-PCR data by geometric averaging of multiple internal control genes. Genome Biol 3:1–12
29. Pfaffl MW, Horgan GW, Dempfle L (2002) Relative expression software tool (REST©) for group-wise comparison and statistical analysis of relative expression results in real-time PCR. Nucleic Acids Res 30:e36
30. Iskar M, Campillos M, Kuhn M, Jensen LJ, van Noort V, Bork P (2010) Drug-induced regulation of target expression. PLoS Comput Biol 6:e1000925
31. Vassiliou GS, Cooper JL, Rad R, Li J, Rice S, Uren A, Rad L, Ellis P, Andrews R, Banerjee R, Grove C, Wang W, Liu P, Wright P, Arends M, Bradley A (2011) Mutant nucleophosmin and cooperating pathways drive leukemia initiation and progression in mice. Nat Genet 43:470–475
32. Mupo A, Celani L, Dovey O, Cooper JL, Grove C, Rad R, Sportoletti P, Falini B, Bradley A, Vassiliou GS (2013) A powerful molecular synergy between mutant nucleophosmin and Flt3-ITD drives acute myeloid leukemia in mice. Leukemia 27:1917–1920
33. Szebeni A, Hingorani K, Negi S, Olson MOJ (2003) Role of protein kinase CK2 phosphorylation in the molecular chaperone activity of nucleolar protein B23. J Biol Chem 278:9107–9115
34. Savkur RS, Olson MOJ (1998) Preferential cleavage in pre-ribosomal RNA by protein B23 endoribonuclease. Nucleic Acids Res 26:4508–4515
35. Maggi LB, Kuchenruether M, Dadey DYA, Schwope RM, Grisendi S, Townsend RR, Pandolfi PP, Weber JD (2008) Nucleophosmin serves as a rate-limiting nuclear export chaperone for the Mammalian ribosome. Mol Cell Biol 28:7050–7065
36. Li X, Rao V, Jin J, Guan B, Anderes KL, Bieberich CJ (2012) Identification and validation of inhibitor-responsive kinase substrates using a new paradigm to measure kinase-specific protein phosphorylation index. J Proteome Res 11:3637–3649
37. Hsieh AC, Costa M, Zollo O, Davis C, Feldman ME, Testa JR, Meyuhas O, Shokat KM, Ruggero D (2010) Genetic dissection of the oncogenic mTOR pathway reveals druggable addiction to translational control via 4EBP-eIF4E. Cancer Cell 17:249–261
38. Dennis PB, Fumagalli S, Thomas G (1999) Target of rapamycin (TOR): balancing the opposing forces of protein synthesis and degradation. Curr Opin Genet Dev 9:49–54
39. Meyuhas O (2000) Synthesis of the translational apparatus is regulated at the translational level. Eur J Biochem 267:6321–6330
40. Chedin S, Laferte A, Hoang T, Lafontaine DL, Riva M, Carles C (2007) Is ribosome synthesis controlled by pol I transcription? Cell Cycle 6:11–15
41. Opferman JT, Zambetti GP (2006) Translational research? ribosome integrity and a new p53 tumor suppressor checkpoint. Cell Death Differ 13:898–901
42. http://p53.iarc.fr/TP53GeneVariations.aspx?mutant=R249S. Accessed 9 Oct 2014
43. Thomas G (2000) An encore for ribosome biogenesis in the control of cell proliferation. Nat Cell Biol 2:E71–E72
44. Schwanhausser B, Busse D, Li N, Dittmar G, Schuchhardt J, Wolf J, Chen W, Selbach M (2011) Global quantification of mammalian gene expression control. Nature 473:337–342
45. Meggio F, Pinna LA (2003) One-thousand-and-one substrates of protein kinase CK2. FASEB J 17:349–368